RSC Advances

COMMUNICATION

View Article Online
View Journal | View Issue

Cite this: *RSC Adv.*, 2014, **4**, 31851

Received 11th May 2014
Accepted 1st July 2014

DOI: 10.1039/c4ra04400b

www.rsc.org/advances

Microwave synthesis of high rate nanostructured $LiMnBO_3$ with excellent cyclic behavior for lithium ion batteries

Kaliyappan Karthikeyan*[ab] and Yun Sung Lee*[b]

$LiMnBO_3$ nanobeads (LMB-NB) prepared using a urea assisted microwave irradiation method delivered 67 mA h g^{-1} capacity at 0.6 C rate between 1.25 and 4.8 V, showing 88% cyclability after 100 cycles. In addition, the LMB-NB electrode also showed superior rate capability with 63 and 55 mA h g^{-1} capacity at 1.5 and 4 C rates, which is the best ever reported rate performance for a $LiMnBO_3$ material.

Recently, much effort has been made to replace layered $LiCoO_2$ cathode materials for large scale lithium ion battery (LIB) application. In spite of considering other layered $LiMO_2$ materials (M = Ni and Mn), $Li(Mn_{1/3}Ni_{1/3}Co_{1/3})O_2$ olivine type material, Li_2MnO_3, $LiMn_2O_4$ and $LiNi_{0.5}Mn_{1.5}O_2$ as possible alternatives, these materials have their own shortcomings, which prevent them from being applied in LIBs for electric and hybrid electric vehicles.[1–3] Consequently, it is also very important to develop energy sources materials with desirable features like less toxicity, low cost, large theoretical capacity, high chemical and thermal stability. Moreover, the progress of exploring new energy source materials along with high electrochemical performance is also a major challenge for the advancement of LIB in future.[4]

In this line of research, lithium metal borates ($LiMBO_3$, M = Mn or Fe) is attracting more researchers due to the stable polyanion group, high thermal stability, comparable density, electrochemical stability because of small volume changes and its higher theoretical capacity (<220 mA h^{-1}) than other electrode materials like $LiMO_2$ (M = Co, Ni, Mn and Fe) and $LiFePO_4$.[5] In addition, boron is naturally abundant and environmentally benign. Further, triangle $(BO_3)^{3-}$ polyoxanions also has lighter mass compared to other polyoxanion groups $(XO_m)^{n-}$ reported for LIB such as $(AsO_4)^{2-}$, $(VO_4)^{2-}$, $(SO_4)^{2-}$, $(WO_4)^{2-}$, $(PO_4)^{2-}$, and $(SiO_4)^{2-}$. In addition, $(BO_3)^{3-}$ polyoxanions could deliver high output potential along with improved structural stability from inductive effect of B–O bond. Although $LMBO_3$ exhibited higher operating voltage and enhanced structural stability by keeping the benefit of networking anion group, they were suffered from low electrical conductivity similar to those of the olivine framework. The electrochemical activity of $LMBO_3$ was initially reported by Legagneur *et al.* along with low electrochemical activity.[5] While considering $LiFeBO_3$ is safer than $LiMnBO_3$, high capacity and high redox potential (~4.6 V) than that of $LiFeBO_3$ (~3.2 V) makes $LiMnBO_3$ as more attractive candidate for LIB. Generally, $LiMnBO_3$ (LMB) exists in two polymorphs, which is either hexagonal (h-LMB) or monoclinic (m-LMB) phases.[6] It was reported by several researchers that m-LMB exhibited better electrochemical reactivity than h-LMB.[6–8] Kim *et al.* observed high capacity of ~100 mA h g^{-1} for m-LMB at low current density of C/20 in the second cycle.[6] Of late, several efforts had been taken to improve the electrochemical performance of LMB using carbon coating or making them composite with graphene.[7–11] Although the electrochemical activity of LMB was increased at low current densities, the high current rate performance is still not satisfactory to adopt them in large scale applications. It is well known that synthesis method played an important role to enhance the morphological feature thereby improving Li-ion storage behavior.[7,10,11] Apparently, utilization of nano-LMB, which reduced the pathway for Li-ion diffusion through its size effect and hence enhanced rate capability could be achieved. Moreover, forming highly conductive network between the nano-LMB is also an effective way to improve its inherent conductive properties and electrochemical reaction kinetics as well.[12] In this work, we have prepared monoclinic LMB nanobeads with ultra-thin carbon conductive network (LMB-NB) using urea assisted microwave irradiation method. Nevertheless, development of LMB-NB *via* microwave method has not been reported yet. The prepared materials had showed remarkable cycling performance even at high current rates, which is the best performance reported so far for LMB.

[a]*Department of Mechanical and Materials Engineering, The University of Western Ontario, London, Ontario, N6A 5B9, Canada. E-mail: kkaliyap@uwo.ca; leeys@chonnam.ac.kr*

[b]*Faculty of Applied Chemical Engineering, Chonnam National University, Gwang-ju 500-757, Korea*

Monoclinic LMB-NB were prepared using microwave irradiation method with urea as surfactant as well as carbon sources. Stoichiometric amounts of lithium nitrate, manganese nitrate and boric acid were dissolved in 100 mL of distilled water. Then, an appropriate amount of urea was added to the above solution and stirred for 90 min. The molar ratio of metal ions to urea was fixed at 1 : 10. The resulting solution was heated in a domestic microwave oven (700 W, Daewoo, Korea) for 20 min, and then cooled to room temperature. Finally, the resultant product was fired at 650 °C for 7 h in an argon atmosphere to obtained LMB-NB powders. The phase analysis of LMB-NB was examined through X-ray diffraction measurements (XRD, Rint 1000, Rigaku, Japan) equipped with Cu-Kα as the radiation source. The morphological behavior of the LMB-NB was examined using a field emission transmission electron microscope (TEM, Tecnai-F20, Philips, Netherland). Brunauer–Emmett–Teller (BET) surface area analysis was performed using an ASAP 2010 surface analyzer (Micromeritics, USA). The amount of carbon content in LMB-NB was determined by thermogravimetric analysis (TGA) from ambient temperature to 500 °C using a thermal analyzer system (STA 1640, Stanton Redcroft Inc., UK). The electrochemical performance individual LMB-NB was tested against a lithium counter electrode. The electrodes for half-cell were prepared by pressing a slurry of 80% active material, 10% ketzen black (KB) as conductive additive, and a 10% Teflonized acetylene black (TAB with 7 wt% of Teflon) binder on a 200 mm^2 nickel mesh and dried at 160 °C for 4 h in an oven. The half-cells were fabricated in an argon filled glove box by sandwiching together a LMB-MB cathode and lithium anode separated by a separator (Celgard 3401) in 1 M $LiPF_6$ in a mixture of ethylene carbonate (EC) and dimethyl carbonate (DMC) (1 : 1 v/v, Soulbrain Co., Ltd, Korea) electrolyte. Electrochemical impedance spectroscopy (EIS) measurements were carried out using an electrochemical analyzer (SP-150, Bio-Logic, France). The charge–discharge test (C–DC) was performed in CR2032 type cell. The cathodes for the coin cell were prepared by pressing the mixture of 77% LMB-NB, 11.5% of Ketjen black and 11.5% of Teflonized acetylene black (TAB) mixture on 150 mm^2 nickel mesh and dried at 160 °C for 4 h in a vacuum oven. The test cells were fabricated in an argon filled glove box by pressing a cathode and lithium metal anode separated by a porous polypropylene separator (Celgard 3401). 1 M $LiPF_6$ in 1 : 1 EC–DMC (v/v) was used as electrolyte.[12]

Fig. 1a presented the XRD pattern of LMB-NB, which could be indexed based on monoclinic phase with *C*2/*c* space group according to the JCPDS card no. 83-2342.[5] Furthermore, narrow and highly indexed XRD peaks confirmed good crystalline nature of LMB-NB powders. The cell parameters $a = 5.192$ Å, $b = 8.944$ Å and $c = 10.328$ Å were observed and in good agreement with m-LMB.[10] In addition, the average crystallite size of powders grown by microwave irradiation method was found to be ~40 nm using Scherrer's formula. The presence of Mn^{2+} in LMB-NB was confirmed using electron paramagnetic resonance (EPR) as presented in Fig. 1b. The EPR of LMB-NB showed single broad line centered at 310.025 mT $g \sim 2.00$, indicating the existence of manganese ions in 2^+ state.[13]

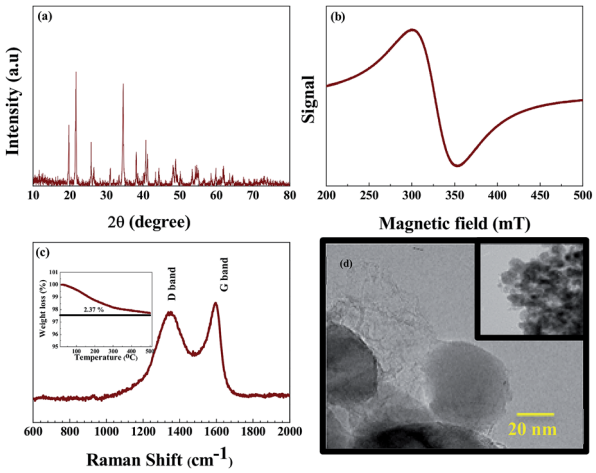

Fig. 1 (a) XRD pattern, (b) ESR, (c) Raman spectra and (d) TEM of LMB-NB prepared using urea assisted microwave irradiation method at 600 °C.

The Raman spectrum in Fig. 1c exhibited two broad peaks namely at ~1596 (G-band) and 1347 (D-band) cm^{-1}, which are characteristic for graphitic nature of carbon. The G-band originates from symmetric E_{2g} vibrations mode of sp^2 atoms whereas the D-band is corresponds to the breathing mode of *k*-point phonons of A_{1g} symmetry. The prominent peak at 1596 cm^{-1} can be attributed to disordered sp^3 bonded graphitic carbon, facilitating the improvement of ionic/electronic transfer of LMB-NB material. The BET surface area and carbon

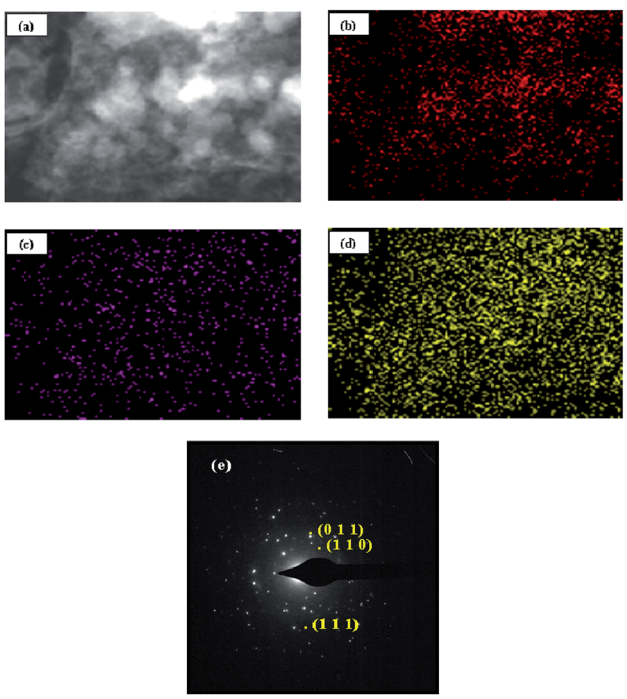

Fig. 2 (a) TEM images of LMB-NB particles, (b) mapping of Mn, (c) mapping of B, (d) mapping of c coating layer and (e) SAED pattern of LMB-NB prepared using microwave irradiation method.

content in LMB-NB are calculated about 11 $m^2 g^{-1}$ and 2.37% (inserted in Fig. 1c), respectively. It is clear from TEM image in Fig. 2d that the LMB-NB power was composed of small and highly ordered particles (insert in Fig. 2d) with average grain size of 30–40 nm. Moreover, each particle is interconnected well through ultra-thin porous carbon backbone, resulting from the combustion of urea, which also suppresses the particle growth during the synthesis process. This interconnected carbon network between LMB-NB is not only increases the conductive nature of LMB-NB, it also more allowed to store more electrolyte within LMB-NB structure, augmenting the structural stability against the inherent mechanical stress during the high current cycling process. It is well-known that the electrode material with high number of reaction sites, uniform particles with homogeneous size distribution and stable structure are essential parameters for improving the C–DC capability at high current rate.

The presence of carbon was confirmed using EDX and corresponding dot mapping was showed in Fig. 2. The mapping of Mn in Fig. 2b exhibited similar intensity distribution to B in Fig. 2c, demonstrating the homogeneity of LMB-NBs. Moreover, Fig. 2d showed the presence of homogeneously distributed carbon on the nanobeads. Besides, the selected area electron diffraction (SAED) pattern of LMB-NBs in Fig. 2e displayed bright spots, which could be indexed based on the interplanar spacings according to the monoclinic structure of LMB-NBs.[8]

Fig. 3 represented the initial charge–discharge (C–DC) curves of the cells cycled between 1.25–4.8 V under ambient temperature at a C/20 rate. As seen from Fig. 3 that the LMB-NB showed the sloped C–DC behaviour, in accordance with the other reports on the monoclinic LMB cathode.[11] The charge profile of LMB-NB revealed that about 0.75 mole of Li^+ could be extracted from its structure at C/20 current rate up to 4.8 V, corresponding to the capacity of ~166 mA h g^{-1}. During discharge, ~0.54 mole of Li^+ was reinserted into the LMB-NB structure, delivering a discharge capacity of ~120 mA h g^{-1}. It is clear that there was some irreversible capacity loss during the initial cycle, which may be attributed to the formation of solid-electrolyte interface film on the surface of the electrode material and electrolyte decomposition at high voltage.[5,14]

The discharge curves of Li^+/LMB-NB cell recorded within 1.25–4.8 V at different current densities are illustrated in Fig. 4a. The trend of C–DC curves are in well agreement with previous reports on LMB cathodes.[10,11] Since $(BO_3)^{3-}$ polyanion has strong covalent bonding with metal ions, the high redox potential of $Mn^{3+/2+}$ couple could be resulted from the alternating the $Mn^{3+/2+}$ couple by polyanion.[5,14] It well known that the lithium intercalation reaction kinetics at high current densities is low due to the reduced Li-ion diffusion process, since at high current rates the Li-ions approach only the outer surface of the electrode material. This is based on the diffusion effects of the Li-ion within the electrode material. Hence, it is held that part of the surface of the electrode materials contribute to a high charging–discharging rate, which decreased the voltage plateau at higher current rates, resulting low capacity value.[12] Although all the cells showed irreversible capacity loss during the initial cycle at all current densities, the columbic efficiency of the cell is over 96% upon cycling process. A discharge capacities of 67, 64 and 55 mA h g^{-1} can be obtained at a current rate of 0.6, 1.5 and 4 C, respectively from Li^+/LMB-NB cell.

It is worth mentioning here that the capacity obtained in the present investigation is one of the best ever reported values for LMB cathode especially at high current rates.[5–7,10,11,15] This superior electrochemical lithium storage performance is resulted from its morphological feature. The uniformly distributed LMB-NB along with ultra-thin porous carbon backbone could facilitate the Li-ion diffusion even at high current rates. On the other hand, nano sized LMB-NB also improved the contact between the particles–particles and the particles–current

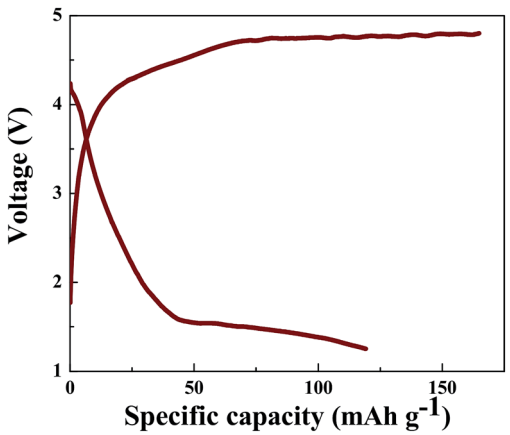

Fig. 3 Initial C–DC curve of LMB-NB electrode within 1.25–4.8 V at C/20 current rate.

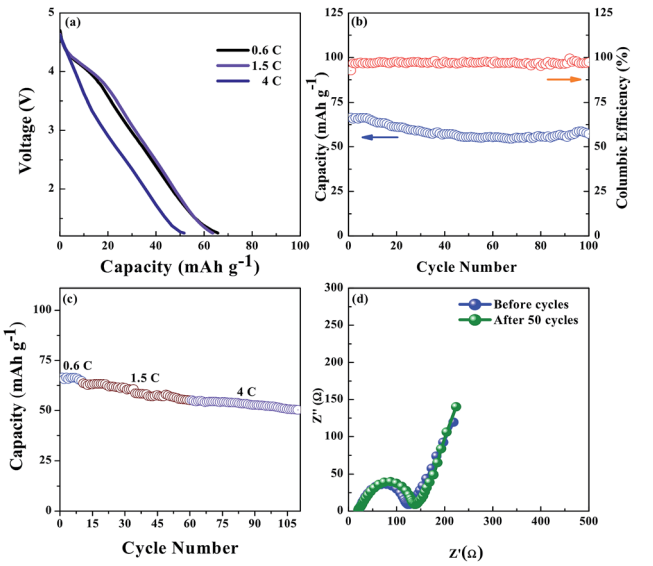

Fig. 4 (a) C–DC curves of Li^+/LMB-NB cell conducted between 1.25 and 4.8 V at different current rates, (b) cyclic performance of Li^+/LMB-NB cell at 0.6 C for 100 cycles, (c) rate capability of Li^+/LMB-NB cell at different current rates and (d) Nyquist spectra of Li^+/LMB-NB cell recorded before and after cycled at 4 C for 50 cycles.

collector, ensuring the improvement of electrical conductivity and hence the lithium ion storage capability was enhanced.

The cycling performance at 0.6 C rate is presented in Fig. 4b. The cell exhibited ~88% capacity retention at 0.6 C rate along with more than 96% of coulombic efficiency. To the best of our knowledge, it is the best cycling performance for LMB powders prepared using various synthesis methods including sol–gel, spray drying, solid state and carbothermal reaction methods.[6–9,11,14] Furthermore, the Li^+/LMB-NB cell also displayed very stable cyclic performance at all current rates as presented in Fig. 4c. As observed from TEM analysis, the formation of ultra-thin porous carbon network between LMB-NB not only improves its conductivity, but also allowed to adsorb more electrolyte through the open carbon matrix and stabilizes the electrode/electrolyte interface, which improved the rate capability. In the meantime, electrolyte adsorption within LMB-NB structure also provided flexible structure against volume expansion/contraction during the cycling progress thus stabilized cycling performance even at high current rates.[12]

Nyquist spectra recorded before and after cycling at 4 C rate for 50 are given in Fig. 4d. As seen from Fig. 3d, the diameter of the semi-circle at low frequency region associated to the charge transfer resistance (R_{ct}) was slightly larger than that of before cycling, revealing that the increase in R_{ct} value before and after cycled at high rate was relatively small. This outstanding cycling behavior at high current could result from the synergetic effect of improved intrinsic electronic and mechanical properties of the LMB-NB supported by ultra-thin porous carbon network, which correlated well with the results obtained from C–DC studies. Furthermore, negligible agglomeration and high crystalline nature of LMB-NB also aided the charge storage of Li^+/LMB-NB cell. These results clearly demonstrated that urea mediated microwave irradiation method could significantly enhanced both the conductivity and electrochemical reaction kinetics of LMB-NB for high performance LIB applications.

Conclusions

The LMB-NB were synthesised using urea assisted microwave method and the possibility of utilizing them as high performance electrode materials for LIB was investigated against lithium counter electrode between 1.25 and 4.8 V at different current rates. The Li^+/LMB-NB cell delivered a discharge capacities of 67, 63 and 55 mA h g^{-1} at a current rate of 0.6 C, 1.5 C and 4 C, respectively along with excellent cyclic stability, which can be considered to be the best rate performance among other reports available on $LiMNBO_3$. The reason for the improved electrochemical performance could be concluded as follows: the formation of highly porous ultra-thin carbon network between LMB-NB particles suppressed the particle agglomeration and increased the conductive nature of the materials as well as stabilized the solid-electrolyte interfacial layer, resulting in the excellent lithium storage behavior of LMB-NB electrode even at high current densities.

Notes and references

1 M. S. Whittingham, *Chem. Rev.*, 2004, **104**, 4271–4302.
2 A. K. Padhi, K. S. Nanjundaswamy and J. B. Goodenough, *J. Electrochem. Soc.*, 1997, **144**, 1188–1194.
3 V. Aravindan, J. Gnanaraj, Y.-S. Lee and S. Madhavi, *J. Mater. Chem. A*, 2013, **1**, 3518–3539.
4 P. G. Bruce, B. Scrosati and J.-M. Tarascon, *Angew. Chem., Int. Ed.*, 2008, **47**, 2930–2946.
5 V. Legagneur, Y. An, A. Mosbah, R. Portal, A. Le Gal La Salle, A. Verbaere, D. Guyomard and Y. Piffard, *Solid State Ionics*, 2001, **139**, 37–46.
6 J. C. Kim, C. J. Moore, B. Kang, G. Hautier, A. Jain and G. Ceder, *J. Electrochem. Soc.*, 2011, **158**, A309–A315.
7 Y.-S. Lee and H. Lee, *Electron. Mater. Lett.*, 2014, **10**, 253–258.
8 S. Afyon, D. Kundu, F. Krumeich and R. Nesper, *J. Power Sources*, 2013, **224**, 145–151.
9 R. Ma, L. Shao, K. Wu, M. Lao, M. Shui, C. Chen, D. Wang, N. Long, Y. Ren and J. Shu, *Ceram. Int.*, 2013, **39**, 9309–9317.
10 K.-J. Lee, L.-S. Kang, S. Uhm, J. S. Yoon, D.-W. Kim and H. S. Hong, *Curr. Appl. Phys.*, 2013, **13**, 1440–1443.
11 V. Aravindan, K. Karthikeyan, S. Amaresh and Y. S. Lee, *Bull. Korean Chem. Soc.*, 2010, **31**, 1506–1509.
12 K. Karthikeyan, S. Amaresh, V. Aravindan, W. S. Kim, K. W. Nam, X. Q. Yang and Y. S. Lee, *J. Power Sources*, 2013, **232**, 240–245.
13 L. Pawlak, K. Falkowski and S. Pokrzywnicki, *J. Solid State Chem.*, 1981, **37**, 228–231.
14 L. Chen, Y. Zhao, X. An, J. Liu, Y. Dong, Y. Chen and Q. Kuang, *J. Alloys Compd.*, 2010, **494**, 415–419.
15 S. Li, L. Xu, G. Li, M. Wang and Y. Zhai, *J. Power Sources*, 2013, **236**, 54–60.

